Comparative evaluation of the impact of WRF/NMM and WRF/ARW meteorology on CMAQ simulations for PM$_{2.5}$ and its related precursors during the 2006 TexAQS/GoMACCS study

Shaocai Yu, Rohit Mathur, Jonathan Pleim, George Pouliot, David Wong, Brian Eder,

Kenneth Schere, Rob Gilliam, and S.T. Rao

Atmospheric Modeling and Analysis Division
National Exposure Research Laboratory, U.S. Environmental Protection Agency,

Research Triangle Park, NC 27711

Revision on 3/2/2012

Abstract

This study presents a comparative evaluation of the impact of WRF-NMM and WRF-ARW meteorology on CMAQ simulations of $PM_{2.5}$, its composition and related precursors over the eastern United States with the intensive observations obtained by aircraft (NOAA WP-3), ship and surface monitoring networks (AIRNow, IMPROVE, CASTNet and STN) during the 2006 TexAQS/GoMACCS study. The results at the AIRNow surface sites show that both ARW-CMAQ and NMM-CMAQ reproduced day-to-day variations of observed $PM_{2.5}$ and captured the majority of observed $PM_{2.5}$ within a factor of 2 with a NMB value of -0.4% for ARW-CMAQ and -18% for NMM-CMAQ. Both models performed much better at the urban sites than at the rural sites, with greater underpredictions at the rural sites. Both models consistently underestimated the observed $PM_{2.5}$ at the rural IMPROVE sites by -1% for the ARW-CMAQ and -19% for the NMM-CMAQ. The greater underestimations of SO_4^{2-}, OC and EC by the NMM-CMAQ contributed to increased underestimation of $PM_{2.5}$ at the IMPROVE sites. The NMB values for $PM_{2.5}$ at the STN urban sites are 15% and -16% for the ARW-CMAQ and NMM-CMAQ, respectively. The underestimation of $PM_{2.5}$ at the STN sites by the NMM-CMAQ mainly results from the underestimations of the SO_4^{2-}, NH_4^+ and TCM components, whereas the overestimation of $PM_{2.5}$ at the STN sites by the ARW-CMAQ results from the overestimations of SO_4^{2-}, NO_3^-, and NH_4^+. The Comparison with WP-3 aircraft measurements reveals that both ARW-CMAQ and NMM-CMAQ have very similar model performance for vertical profiles for $PM_{2.5}$ chemical components (SO_4^{2-}, NH_4^+) and related gaseous species (HNO_3, SO_2, NH_3, isoprene, toluene, terpenes) as both models used the same chemical mechanisms and emissions. The results of ship along the coast of southeastern Texas over the Gulf of Mexico show that both models captured the temporal variations and broad synoptic change seen in the observed HCHO and acetaldehyde with the means NMB <30% most of the time but they consistently underestimated terpenes, isoprene, toluene and SO_2.

1. Introduction

Fine particulate matter (PM$_{2.5}$, particles with aerodynamic diameters less than 2.5 μm) results from primary direct emissions and secondary formation through atmospheric oxidation of gaseous precursors such as sulfur oxides (SO$_x$), nitrogen oxides (NO$_x$) and volatile organic compounds (VOCs), and subsequent gas-to-particle conversion processes. To reflect more recent health effect studies and provide increased protection of public health and welfare, the level of the 24-h PM2.5 National Ambient Air Quality Standards (NAAQS) has been revised from 65 μg m^{-3} to 35 μg m^{-3}, effective on 18 December 2006 (Federal Register, 2006). The rationale for this revision includes consideration of: (1) Evidence of health effects related to short- and long-term exposures to fine particles; (2) insights gained from a quantitative risk assessment; and (3) specific conclusions regarding the need for revisions to the current standards and the elements of PM$_{2.5}$ standards (i.e., indicator, averaging time, form, and level) that, taken together, are requisite to protect public health with an adequate margin of safety (Federal Register, 2006). Unlike O$_3$ pollution which occurs typically during the high pressure, hot, sunny and stagnant atmospheric conditions at the locations with substantial VOC and NO$_x$ concentrations, elevated PM$_{2.5}$ concentrations occur throughout the year because PM$_{2.5}$ is composed of a variety of particles differing in size and chemical composition and also because source emissions of each component of the atmospheric particles vary differently and seasonally. For example, sulfate is produced from both primary and secondary sources but elemental carbon (EC) is emitted from the primary sources. Differences in the composition of particles produced by different sources lead to spatial and temporal heterogeneity in the composition of the atmospheric aerosols.

The relationship between PM$_{2.5}$ and meteorological conditions has been examined by several studies (Whiteaker et al., 2002; Wehner and Wiedensohler, 2003; Wise and Comrie, 2005; Dawson et al., 2007). The meteorological conditions can have complex effects on the concentrations of PM$_{2.5}$ due to the fact that PM$_{2.5}$ is comprised of many different species and the meteorological impacts on individual species are different. For example, in the study of sensitivity of PM$_{2.5}$ to various meteorological parameters in the eastern U.S., Dawson et al. (2007) showed that the strongest effects of changes in

meteorology on $PM_{2.5}$ concentrations were from temperature, wind speed, absolute humidity, mixing height and precipitation effects, whereas cloud liquid water content, optical depth and cloudy area can lead to small changes in $PM_{2.5}$ on average with appreciable responses in some areas. The changes in concentrations of $PM_{2.5}$ caused by changes in meteorology should be taken into account in long-term air quality management as concluded by them.

The 2006 Texas Air Quality Study / Gulf of Mexico Atmospheric Composition and Climate Study (TexAQS/GoMACCS) was a joint regional air quality and climate change study conducted during the late summer (August 1 to October 15, 2006). The objective of the program is to provide a better understanding of the sources and atmospheric processes responsible for the formation and distribution of ozone and aerosols in the atmosphere, their impact on human health and regional haze as well as the influence on the radiative forcing of climate over Texas and the northwestern Gulf of Mexico. The comprehensive observational data from the 2006 TexAQS/GoMACCS can be used to examine in detail the performance of air quality models from a multipollutant perspective, in terms of their surface concentrations as well as vertical distributions. In this study, we examine the impact of these two different meteorological fields (WRF-ARW and WRF-NMM) on the CMAQ simulations for $PM_{2.5}$, its chemical composition and precursors. The purpose of this paper is to comparatively examine the impact of these two different meteorological fields on CMAQ simulations for vertical profiles of $PM_{2.5}$, its chemical composition and precursors on the basis of the extensive measurements obtained by aircraft and ship during the 2006 TexAQS/GoMACCS field experiment, especially, for three types of plumes (power plant plumes, Houston and Dallas urban plumes and Ship Channel plumes) over the Houston-Galveston-Brazoria and Dallas-Fort Worth (DFW) metropolitan areas. The influence of these two different meteorological fields on spatial and temporal variations of $PM_{2.5}$, and its chemical composition over the eastern U.S. is also evaluated against the observations from the surface monitoring networks (AIRNOW, IMPROVE, CASTNet and STN) during the 2006 TexAQS/GoMACCS study.

2. Description of the modeling system and observational databases
2.1. Description of the modeling system

The detailed description of the modeling system and configurations is given by Yu et al. (2011). Here a brief summary relevant to the present study is presented. The WRF model is a state-of-science mesoscale model framework with two available dynamic cores: the Non-hydrostatic Mesoscale Model (NMM) developed by NCEP (Janjic, 2003) and the Advanced Research WRF (ARW) developed by NCAR (Skamarock et al., 2005). These two dynamic cores cannot be merged because each dynamic core corresponds to a set of dynamic solvers that operates on a particular grid projection, grid staggering and vertical coordinate (Skamarock, 2005). As summarized by Skamarock (2005), operational results indicated that the significant differences between these two dynamic core forecasts are more the result of different physics but not dynamical core designs. The NMM core is a fully compressible hydrostatic NWP (Numerical Weather Prediction) model using mass based vertical coordinate, which has been extended to include the non-hydrostatic motions (Janjić, 2003), whereas the ARW core is a fully compressible, Eulerian nonhydrostatic model with a run-time hydrostatic option available. The NMM core uses a terrain-following hybrid (sigma-pressure) vertical coordinate and Arakawa E-grid staggering for horizontal grid, whereas the ARW core uses a terrain-following hydrostatic-pressure vertical coordinate with vertical grid stretching permitted and Arakawa C-grid staggering for horizontal grid. As summarized in Yu et al. (2011), the physics package of the NMM (ARW) includes the Betts-Miller-Janjic (Kain-Fritsch (KF2)) convective mixing scheme, Mellor-Yamada-Janjic (Asymmetric Convective Model (ACM2)) planetary boundary layer (PBL) scheme, Lacis-Hansen (Dudhia) shortwave and Fels-Schwartzkopf (RRTM) longwave radiation scheme, Ferrier (Thompson) cloud microphysics, and NOAH (Pleim-Xiu (PX)) land-surface scheme. In this study, both WRF-ARW and WRF-NMM are employed to provide meteorological fields for CMAQ (the notations ARW-CMAQ and NMM-CMAQ will be used hereafter to represent these two configurations). NMM-CMAQ uses the lowest 22 layered vertical grid structure of the 60 hybrid layers in WRF-NMM meteorological fields directly without vertical interpolation through the use of a common vertical coordinate system. On the other hand, the WRF-ARW model has been employed to generate meteorological fields for CMAQ because the WRF-ARW meteorological model is compatible with CMAQ like MM5 before. For the NMM-CMAQ run, the results from the target forecast

period (0400 UTC to next day's 0300 UTC) based on the 1200 UTC NMM-CMAQ simulation cycle over the domain of the continental United States (see Figure 1a of Yu et al. (2011)) are used, whereas the ARW-CMAQ model with 34 vertical layers was applied over a domain encompassing the eastern United States (see Figure 1b of Yu et al. (2011)) and was run from the beginning to end with first three days as model spin-up over the whole period.

Given the fact that both models use different map projections and grid staggering, it is difficult to make the WRF-ARW grid coverage identical to the WRF-NMM coverage. Several steps are taken to ensure that both the models are set up as consistently as possible so that the comparison of the two models is meaningful. First, the meteorological fields of ARW were padded by 5 cells in both x and y directions around the original meteorological domain when the meteorological fields were processed using Meteorology-Chemistry Interface Program (MCIP) to create the CMAQ-ready files. This helps match the larger NMM domain and smaller ARW domain sizes, and is able to use the emission data from the NMM-CMAQ forecast model. Second, the point source emissions were redistributed to the 34 layers according to the ARW meteorological fields on the basis of those from the NMM-CMAQ model. In addition, the ARW-CMAQ uses the same area sources such as the mobile and biogenic sources as those in NMM-CMAQ. Therefore, the total emission budgets for both models are the same. In both ARW-CMAQ and NMM-CMAQ, the lateral boundary conditions are horizontally constant and are specified by continental ''clean'' profile for O_3 and other trace gases; the vertical variations are based on climatology (Byun and Schere, 2006). For both models, the thickness of layer 1 is about 38 m and the vertical coordinate system resolves the atmosphere between the surface and 50 hPa although each model uses different number of vertical levels.

The Carbon Bond chemical mechanism (version 4.2) has been used to represent photochemical reaction pathways in both NMM-CMAQ and ARW-CMAQ. The area source emissions are based on the 2001 National Emission Inventory. The point source emissions are based on the 2001 Continuous Emission Monitoring estimates of SO_2 and NO_x projected to 2006 on a regional basis using the Department of Energy's 2006 Annual Energy Outlook issued in January of 2006 (DOE, 2006). The mobile source emissions

were generated by EPA'S MOBILE6 model using 1999 Vehicle Miles Traveled data and a fleet year of 2006.

The aerosol module in CMAQ is described by Binkowski and Roselle (2003) and updates are described by Bhave et al. (2004) and Yu et al. (2007). The size distribution of aerosols in tropospheric air quality models can be represented by the sectional approach (Zhang et al., 2004), the moment approach (Yu et al., 2003), and the modal approach (Binkowski and Roselle, 2003). In the aerosol module of CMAQ, the aerosol distribution is modeled as a superposition of three lognormal modes that correspond nominally to the ultrafine (diameter (Dp) < 0.1 mm), fine (0.1 < Dp < 2.5 mm), and coarse (Dp > 2.5 mm) particle size ranges. Each lognormal mode is characterized by total number concentration, geometric mean diameter and geometric standard deviation. The model results for $PM_{2.5}$ concentrations are obtained by summing aerosol species concentrations over the first two modes. Generally speaking, the modal approach offers the advantage of being computationally efficient, whereas the sectional representation provides more accuracy at the expense of computational cost. The CMAQ model is able to simulate the integral properties of fine particles such as $PM_{2.5}$ mass and visible aerosol optical depth well but it cannot resolve PM size distributions accurately (Yu et al., 2008). In this study, we only present the model performance for $PM_{2.5}$ mass but not size distributions.

2.2. Observational databases

Four surface monitoring networks for PM2.5 measurements were employed in this evaluation (Interagency Monitoring of Protected Visual Environments (IMPROVE), Speciated Trends Network (STN), Clean Air Status Trends Network (CASTNet) and Air Quality System (AQS)), each with its own and often disparate sampling protocol and standard operating procedures. In the IMPROVE network, two 24-h samples are collected on quartz filters each week, on Wednesday and Saturday, beginning at midnight local time (Sisler and Malm, 2000). The observed $PM_{2.5}$, SO_4^{2-}, NO_3^-, EC and OC data are available at 71 rural sites across the eastern United States. The STN network (http://www.epa.gov/air/data/aqsdb.html) follows the protocol of the IMPROVE network (i.e., every third day collection) with the exception that most of the sites are in urban

areas. The observed $PM_{2.5}$, SO_4^{2-}, NO_3^-, and NH_4^+ data are available at 178 STN sites within the model domain. The CASTNet (http://www.epa.gov/castnet/) collected the concentration data at predominately rural sites using filter packs that are exposed for 1-week intervals (i.e., Tuesday to Tuesday). The aerosol species at the 34 CASTNet sites used in this evaluation include: SO_4^{2-}, NO_3^-, and NH_4^+. The hourly near real-time $PM_{2.5}$ data at 309 sites in the eastern United States are measured by tapered element oscillating microbalance (TEOM) instruments at the U.S. EPA's Air Quality System (AQS) network sites. In addition, measurements of vertical profiles of $PM_{2.5}$, its related chemical composition and gas species (CO, NO, NO_2, HNO_3, PAN, ethylene), and meteorological parameters (liquid water content, water vapor, temperature, wind speed and direction, and pressure) were carried out by instrumented aircraft (NOAA WP-3) and a research ship deployed as part of the 2006 TexAQS/GoMACCS field experiment. The detailed instrumentation and protocols for measurements are described at http://esrl.noaa.gov/csd/2006/fieldops/mobileplatforms.html. The overview of data quality and the principal findings from the 2006 TexAQS/GoMACCS field experiment is given by Parris et al. (2009). The flight tracks of the WP-3 aircraft, and ship movements are presented in Figure 2 of Yu et al. (2011). The results for comparison of the impact of two meteorological models on CMAQ simulations over the eastern U.S. (e.g., ARW domain as shown in Figure 1b of Yu et al. (2011)) during the period of August 6 and October 6 2006 are presented in this study.

3. Results and discussions

3.1. Impact of meteorology on spatial and temporal variations of PM2.5 over the eastern U.S. domain at the AQS sites

Table 1 summarizes the comparison results of the ARW-CMAQ and NMM-CMAQ for the daily (24-h) average $PM_{2.5}$ concentrations. Following the protocol of the IMPROVE network, the daily (24-h) $PM_{2.5}$ concentrations at the AQS sites were calculated from midnight to midnight local time of the next day on the basis of hourly $PM_{2.5}$ observations. The evaluation results at the urban and rural sites are also summarized in Table 1. The domain wide mean values of mean bias (MB) and root mean square error (RMSE) (Yu et al., 2006) for all daily $PM_{2.5}$ at the AQS sites during the

2006 TexAQS/GoMACCS period are -0.1 (-2.3) and 7.9 (7.6) µg m^{-3} for ARW-CMAQ (NMM-CMAQ), respectively, and those for normalized mean bias (NMB) and normalized mean error (NME) are -0.4 (-18.4) % and 43.7 (44.3) % for ARW-CMAQ (NMM-CMAQ), respectively. It is of interest to note that both models performed much better at the urban sites than at the rural sites, with greater underpredictions at the rural sites. As shown in section 3.2, the underestimation of PM$_{2.5}$ at the STN urban sites by the NMM-CMAQ mainly results from the underestimations of the SO$_4^{2-}$, NH$_4^+$ and TCM components, whereas the overestimation of PM$_{2.5}$ at the STN sites by the ARW-CMAQ results from the overestimations of SO$_4^{2-}$, NO$_3^-$, NH$_4^+$, and OTHER.   The greater underestimations of SO$_4^{2-}$, OC and EC by the NMM-CMAQ led to more underestimation of PM$_{2.5}$ at the IMPROVE rural sites. Since TEOM measurements for PM$_{2.5}$ at the AQS sites should be considered as lower limits because of volatilization of soluble organic carbon species in the drying stages of the measurement   (Grover et al., 2005), the underprediction by the model is likely more severe than this evaluation suggests.

Additional insight into the negative bias (underestimation) and errors (scatter) of both models can be gained from Figure 1a for the scatter plot and Figure 1b for the NMB values as a function of the different observed PM$_{2.5}$ concentration ranges. Table 1 and Figure 1 depict that the model performance for ARW-CMAQ and NMM-CMAQ is similar and reasonable for the PM$_{2.5}$ concentration with very close values of RMSE, NME, and correlation coefficient for both models although the ARW-CMAQ has the slightly better performance on the basis of values of MB and NMB. Figures 1a and 1b clearly indicate that both ARW-CMAQ and NMM-CMAQ models reproduced the majority (78%) of the observed daily PM$_{2.5}$ concentrations within a factor of 2, especially for the concentration range of 10 to 35 µg m^{-3}. However, both models overestimated the observations in the low PM$_{2.5}$ concentration range (<10 µg m^{-3}) with NMB values of 37.8% (ARW-CMAQ) and 15.6% (NMM-CMAQ), respectively, but underestimates the observations in the high PM$_{2.5}$ concentration range (>10 µg m^{-3}) consistently. The small NMB value (-0.4%) for the ARW-CMAQ model results from the compensation error between large PM$_{2.5}$ overestimation for low PM$_{2.5}$ concentration portion (<10 µg m^{-3}) and underestimation of high PM$_{2.5}$ concentration portion (>10 µg m^{-3}) as indicated in Figure

1b. The spatial distributions of NMB values for ARW-CMAQ (Figure 1c) and NMM-CMAQ (Figure 1d) show that both models had large underestimation of the observed daily $PM_{2.5}$ concentrations in the southeast, especially for the NMM-CMAQ.   To investigate the model performance over time, the values of mean, MB, RMSE, NMB, NME and correlation coefficient (r) were calculated (domain wide averages) and plotted as daily time series for the daily $PM_{2.5}$ concentrations as shown in Figure 2. The NMB values range from -50.4% (23 September) to 18.9% (25 September) for NMM-CMAQ and from -36.8% (7 August) to 41.1% (2 October) for the ARW-CMAQ. Both models had consistently slight underestimations of $PM_{2.5}$ for the first period from 6 August to 3 September but general overestimations after 3 September. The domain daily mean $PM_{2.5}$ concentrations for the ARW-CMAQ are consistently about 17% higher than those for the NNM-CMAQ during the 2006 TexAQS/GoMACCS period although the RMSE, NME and correlation coefficient values are close for these two models as shown in Figure 2.

3.2. Influence of meteorology on spatial and temporal evaluation for $PM_{2.5}$ and its chemical components at the CASTNet, IMPROVE, STNsites over the eastern U.S

The scatter plots of Figure 3a indicate that at the IMPROVE, CASTNet and STN sites, both ARW-CMAQ and NMM-CMAQ captured a majority of observed SO_4^{2-} (65% (ARW-CMAQ), 74% (NMM-CMAQ)), NH_4^+ (60% (ARW-CMAQ), 69% (NMM-CMAQ)), $PM_{2.5}$ (66% (ARW-CMAQ), 72% (NMM-CMAQ)) concentrations within a factor of 2. The examination of the domain-wide bias and errors (Table 2) for different networks reveals that the NMM-CMAQ consistently underestimated the observed mean SO_4^{2-} by 29%, 18% and 14% at the CASTNet, IMPROVE and STN sites, respectively, whereas the ARW-CMAQ overestimated the observed mean SO_4^{2-} by 16% and 27% at the IMPROVE and STN sites, respectively, with slight underestimation of 10% at the CASTNet site. Both models overestimated the observed NH_4^+ at the STN sites (by 45 % for ARW-CMAQ and 33% for NMM-CMAQ) but underestimated at the CASTNet sites (by -3% for ARW-CMAQ and -22% for NMM-CMAQ).   Both models overestimated the observed SO_2 by more than 80% at the CASTNet sites. The comparison of the modeled and observed total sulfur ($SO_4^{2-}+ SO_2$) at the CASTNet sites in Figure 3b reveals that both models overestimated the observed total sulfur symmetrically and the modeled mean

total sulfur values are higher than the observations by 37% and 21% for ARW-CMAQ and NMM-CMAQ, respectively. This indicates too much SO_2 emission in the emission inventory.

The poor model performance for NO_3^- (see scatter plot in Figure 3a and correlation <0.40 except that at the STN sites for the NMM-CMAQ in Table 2) is related in part to volatility issues of measurements associated with NO_3^-, and their exacerbation because of uncertainties associated with SO_4^{2-} and total NH_4^+ simulations in the model (*Yu, et al.,* 2005). Table 2 indicates that both models underestimated the observed mean OC, EC and TC concentrations at the IMPROVE sites by -11%, -12% and -11% for the ARW-CMAQ, respectively, and by -20%, -28% and -21% for the NMM-CMAQ, respectively. Note that since the STN network used the thermo-optical transmittance (TOT) method to define the split between OC and EC while the IMPROVE and the model emission inventory use the thermo-optical reflectance (TOR) method, only the determination of total carbon (TC=OC+EC) is comparable between these two analysis protocols (*Yu et al.*, 2004). Therefore, Table 2 only lists the performance results for TC comparisons from the STN sites. Both models consistently underestimated the observed TC concentrations at the STN sites by -25% for ARW-CMAQ and -42% for NMM-CMAQ. As pointed out by *Yu et al*. (2007), factors contributing to this underestimation of the modeled OC include: (1) missing sources of primary OC in emission inventory used for the summer, (2) underestimation of secondary OC (SOA) formation such as sources from the oxidation of isoprene and sesquiterpenes (*Edney et al*., 2005) and an aqueous-phase mechanism for SOA formation from the oxidation of VOCs (*Carlton et al*., 2006) that were not yet included in the version of the CMAQ model used here. *Morris et al*. (2006) found that including the SOA formation from sesquiterpene and isoprene improved the CMAQ model performance for OC.

Figure 4 shows comparisons of stacked bar-plots for observed and modeled concentrations for each chemical constituent of $PM_{2.5}$ at the STN sites. Note that "OTHER" species in Figure 4 refers to unspecified anthropogenic mass which comes from the emission inventory of $PM_{2.5}$, i.e., $[PM_{2.5}] = [SO_4^{2-}] + [NH_4^+] + [NO_3^-] + [TCM] + [OTHER]$. Since organic compounds comprising ambient particulate organic mass are largely unknown, an average multiplier is frequently used to convert measurements of

OC (typically reported as μg C/m^3) to organic carbonaceous aerosol mass (OCM). The value of 1.4 has been widely used to estimate particulate organic mass (e.g., *Turpin and Lim* (2001)) from measured OC and is also used in our analysis. The ARW-CMAQ overestimated the observed PM$_{2.5}$ at the STN sites (most of them are located in urban areas) by 15%, whereas the NMM-CMAQ underestimated by -16% as listed in Table 2. The stacked bar-plots of Figure 4 show that the underestimation of PM$_{2.5}$ at the STN sites by the NMM-CMAQ mainly results from the underestimations of the SO$_4^{2-}$, NH$_4^+$ and TCM components, whereas the overestimation of PM$_{2.5}$ at the STN sites by the ARW-CMAQ results from the overestimations of SO$_4^{2-}$, NO$_3^-$, NH$_4^+$, and OTHER although the ARW-CMAQ still underestimated the observed TCM. On the other hand, both models consistently underestimated the observed PM$_{2.5}$ at the IMPROVE sites (most of them are located in rural areas) by -1% for the ARW-CMAQ and -19% for the NMM-CMAQ. The notable underestimations of SO$_4^{2-}$, OC and EC by the NMM-CMAQ led to the underestimation of PM$_{2.5}$ at the IMPROVE sites as shown in Table 2. These results suggest a need to improve accuracy of TCM at both rural and urban sites. On the basis of analysis of the diurnal cycles from the AQS PM$_{2.5}$ monitors and comparison with model median diurnal cycles over the northeastern U.S. during the 2004 ICARTT study, McKeen et al (2007) found some inconsistencies with certain processes within the models and the observations. They found very little diurnal variation in the median observed diurnal cycles at urban and suburban monitor locations. However, significant diurnal variability was exhibited by some models, such as the Eta-CMAQ, that does not capture the decrease of observed PM$_{2.5}$ from 0100 to 0600 LT, indicating a reduced role for aerosol loss during the late night and early morning hours (McKeen et al., 2007). The large scatter in Figure 3a for PM$_{2.5}$ can also arise due to inadequate representation of the diurnal evolution of observed PM$_{2.5}$ by both ARW-CMAQ and NMM-CMAQ.

3.3. Influence of meteorology on vertical profiles for PM2.5 chemical components (SO$_4^{2-}$, NH$_4^+$), and its related gas species from 2006 TexAQS/GoMACCS

To compare the modeled (ARW-CMAQ, NMM-CMAQ) and observed vertical profiles, following Yu et al., (2011), the modeled results were extracted by matching the positions of the aircraft to the model grid indices (column, row and layer). The hourly

resolved modeled outputs were also linearly interpolated to the corresponding observational times. The observed and modeled data pairs were grouped according to the model layer for each day and each flight. The vertical profiles from both models and observations obtained in this manner can be regarded to represent average conditions encountered over the study domain. We refer to these average regional vertical variations as composite vertical distributions in the subsequent discussions. Table 3 summarizes the specific missions and weather conditions encountered for each flight used in this study. WP-3 conducted most of its measurements during the daytime (~0940 to ~1700 LST) except on 29 September when the WP-3 measurements were conducted into night (1345 to 2010 LST). As summarized by McKeen et al. (2009), the WP-3 spent a significant fraction of its allocated flight time between 300 and 700 m above the ground and had 10 daytime flights between 13 and 29 September 2006 which consisted of upwind and downwind transects of the Houston and Dallas urban areas. Figure 5 presents modeled and observed daily composite vertical distributions for $PM_{2.5}$ chemical components (SO_4^{2-}, NH_4^+) and related gaseous species (HNO_3, SO_2, NH_3, VOC (isoprene, toluene, terpene)) during the 2006 TexAQS/GoMACCS period. Mean composite vertical distributions according to the model layer for the models (ARW-CMAQ and NMM-CMAQ) and observations for the whole period are summarized in Table 4.

3.3.1. Vertical profiles of SO_4^{2-}, and NH_4^+

As shown in Figure 5 and Table 4, both ARW-CMAQ and NMM-CMAQ generally estimated SO_4^{2-} well on most days except on 9/16 and 9/21 in which the NMM-CMAQ had consistently high SO_4^{2-}. NMM-CMAQ also has consistently high NH_4^+ on 9/16 and 9/21 relative to both observation and ARW-CMAQ. As analyzed in McKeen et al. (2009), on both 9/15 and 9/21, the air masses originating from western Louisiana merging with the Houston plume with high CO, organic aerosol and EC but relative reduced enhancements of NO_y, SO_2 and toluene were sampled by the WP-3. There was an additional influence of an aged continental air mass from the east or southeast affecting the northeastern Houston with a possible biomass burning signature (McKeen et al., 2009). These characteristics of air masses may make some contribution to the poor performance of NMM-CMAQ for SO_4^{2-} and NH_4^+ on 9/21. Figure 5 and Table 4 reveal

that both models often overestimated NH_4^+ for all altitudes except at layer 1, whereas both models systematically underestimated the NH_3 for all altitudes. The large systematical underestimations of NH_3, in part, result from the general overestimations of NH_4^+ because too much of TNH_4 (e.g., $NH_4^++NH_3$) were put into the aerosol phase by the ISORROPIA thermodynamic model and the model results at low NH_3 concentrations were very sensitive to any errors in SO_4^{2-} and TNH_4 in the simulations (Yu, et al., 2005). On the other hand, both models performed well for observed SO_4^{2-} and NH_4^+ on 9/13 and 9/25 over the DFW region although their concentrations were generally lower than those over the Houston urban and industrial areas as shown in Figure 5. The WP-3 flights sampled the plumes downwind of refining and petrochemical regions outside of Houston, Beaumont-Port Arthur, and the Houston Ship Channel region on 9/15, 9/20 and 9/27, respectively. Both models captured the observed SO_4^{2-} and NH_4^+ in these downwind plumes well as shown in Figure 5. Table 4 also shows that the mean SO_4^{2-} concentration (2.35 $\mu g\ m^{-3}$) of ARW-CMAQ is slightly higher than that of NMM-CMAQ (2.24 $\mu g\ m^{-3}$) although the mean NH_4^+ concentrations are very close for the two models.

3.3.2. Vertical profiles for NH_3, SO_2 and HNO_3

Figure 5 shows the comparison of the modeled and observed daily composite vertical distributions for NH_3, SO_2 and HNO_3. As summarized in Table 4 and Figure 5, both models consistently underestimated NH3 on most days except on 9/25. The mean NH_3 concentrations of observations, ARW-CMAQ and NMM-CMAQ are 1.05, 0.41 and 0.37 ppbv, respectively (see Table 4). As indicated previously, the ISORROPIA thermodynamic model put too much of TNH_4 (e.g., $NH_4^++NH_3$) into the aerosol phase, leading to the systematical underestimations of NH3. The reasonable performance for all aerosol related species (NH_3, HNO_3, NH_4^+ and SO_4^{2-}) on 9/25 seems to cause the reasonable partitioning of TNH_4 between gaseous and aerosol phases. Both models generally estimated HNO_3 well on most days except on 9/15, 9/29 and 10/6 in which both models had consistently high HNO_3 as indicated in Figure 5. The mean observed and modeled SO_2 concentrations are close with general overestimations near ground and general underestimations at high altitudes as indicated in Table 4. The relative reduced enhancements of SO_2 on 9/15 and 9/21 is because the air masses originating from western

14

Louisiana were merged with the Houston plums and influenced by an aged continental air mass from the east or southeast for these two days. Both models seem to capture the observed SO_2 on these days well as shown in Figure 5.

3.3.3. Vertical profiles for terpenes, toluene, and isoprene

As analyzed by Ying and Krishnan (2010), biogenic emissions are the largest contributor to the VOC emissions and are almost an order of magnitude higher than all other sources combined over the southeastern Texas domain. The main anthropogenic VOC sources are from petroleum and other industrial sources, and highway gasoline vehicles. Biogenic monoterpenes and isoprene emission rates are high over the coniferous forests of North America, especially in the summer months (*Guenther et al.*, 2000), providing gas precursors for the formation of biogenic secondary organic aerosols (SOA). Anthropogenic toluene stems predominantly from automotive emissions. In the CMAQ aerosol module, biogenic and anthropogenic SOA occur exclusively by absorptive partitioning of condensable oxidation products of aromatic (mainly toluene) and monoterpene compounds into a pre-existing organic-aerosol phase (*Yu et al.*, 2007).

The model's ability to simulate the composite vertical distributions for isoprene, terpene and toluene, as measured by the WP-3, is illustrated in Figure 5 and summarized in Table 4. Both ARW-CMAQ and NMM-CMAQ have similar performances for these VOC species. In general, both models captured the vertical variation patterns of the observed isoprene quite well on most days, except on 9/13 and 9/15. The summaries in Table 4 indicate that both models have reasonable performance for isoprene at the low altitudes (<2000 m) but completely missed the observed isoprene at the high altitudes (>2000 m). A noticeable discrepancy is the consistent underestimation of terpenes by a factor of 2 to 4 by both models (the mean ARW-CMAQ, NMM-CMAQ and observed terpene concentrations for all data are 10.2, 9.7 and 32.1 ppt, respectively) vertically from the low to high altitudes on most days as shown in Figure 5 and Table 4, especially at the high altitudes (> ~1500 m). On the other hand, both models captured the observed toluene well (the mean ARW-CMAQ, NMM-CMAQ and observed toluene concentrations for all data are 118.0, 113.9 and 127.2 ppt, respectively, see Table 4) although both models had slight overestimation near the ground and underestimation at

the high altitudes (>~2000m). The emission inventory for biogenic emissions of isoprene and monoterpenes is highly uncertain, possibly explaining the general underestimations of isoprene and monoterpenes. Since the underestimations of terpenes will cause underestimation of biogenic SOA, leading to the underestimation of OC, improvement of the VOC emission inventory is recommended in order to provide better model results for these species.

3.4. Influence of meteorology on the time-series over the Gulf of Mexico with the Ronald H. Brown ship observations

The time-series comparisons of the observations and models (ARW-CMAQ and NMM-CMAQ) for PM$_{2.5}$ precursors (NH$_3$, SO$_2$, toluene, isoprene, terpenes, HCHO and acetaldehyde) along the ship tracks (see Figure 2 of Yu et al. (2011)) during the 2006 TexAQS/GoMACCS period are shown in Figure 6 and summarized in Table 5. As mentioned in Yu et al. (2011), most of ship's time was spent sampling along the coast of southeastern Texas over the Gulf of Mexico from August 5 to September 11, 2006. Both models have similar performance for each species as indicated in Table 5. Both models captured the temporal variations and broad synoptic change seen in the observed HCHO and acetaldehyde with the means NMB <30% along the ship track most of the time although with some occasional major excursions (see Figure 6). Like those on the basis of WP-3 observations (see section 3.3), both models underestimated biogenic VOCs, such as terpenes, by more than a factor of 2 and isoprene by more than 30%. On the other hand, both models also underestimated SO$_2$ and toluene which are mainly from anthropogenic sources. Both models also missed most of the peak NH$_3$ concentrations although the means of both models are close to the observations as shown in Table 5 and Figure 6. The rapid increases of observed NH$_3$, SO$_2$, toluene, HCHO and acetaldehyde on 2 September are because the ship was anchored in the Barbour's Cut inlet located off Galveston Bay near Houston Ship Channel. Both models missed most of high concentrations for these species. As analyzed in Yu et al. (2011), the complexity over the coastal region of the Gulf of Mexico with highly variable mixing depth in space and time because of land-sea contrast, the sea-breeze cycle, land-use differences and along-shore

16

coastal irregularities causes both models to be unable to simulate the transport well over land-ocean interface.

4. Conclusions

A detailed evaluation of the impact of WRF-ARW and WRF-NMM meteorology on CMAQ simulations for $PM_{2.5}$, its chemical components and its related precursors has been carried out over the eastern U.S. by comparing the model results with the observations from a variety of surface monitoring networks and aircraft obtained during the 2006 TexAQS/GoMACCS study. The results at the AQS surface sites show that both ARW-CMAQ and NMM-CMAQ reproduced day-to-day variations of observed $PM_{2.5}$ and captured the majority of observed $PM_{2.5}$ within a factor of 2 with the NMB value =-0.4% for ARW-CMAQ and -18.4% for NMM-CMAQ, especially for the concentration range of 10 to 35 μg m^{-3}. The domain daily mean $PM_{2.5}$ concentrations for the ARW-CMAQ are consistently about 17% higher than those for the NNM-CMAQ during the 2006 TexAQS/GoMACCS period although both models performed much better at the urban sites than at the rural sites, with greater underpredictions at the rural sites. On the contrary, the ARW-CMAQ overestimated the observed $PM_{2.5}$ at the STN sites (most of them are located in urban areas) by 15%, whereas the NMM-CMAQ underestimated by -16%. The underestimation of $PM_{2.5}$ at the STN sites by the NMM-CMAQ mainly results from the underestimations of the SO_4^{2-}, NH_4^+ and TCM components, whereas the overestimation of $PM_{2.5}$ at the STN sites by the ARW-CMAQ results from the overestimations of SO_4^{2-}, NO_3^-, NH_4^+, and OTHER. Both models consistently underestimated the observed $PM_{2.5}$ at the IMPROVE sites (most of them are located in rural areas) by -1% for the ARW-CMAQ and -19% for the NMM-CMAQ. The greater underestimations of SO_4^{2-}, OC and EC by the NMM-CMAQ led to increased underestimation of $PM_{2.5}$ at the IMPROVE sites. As shown in Yu et al. (2011), the mean temperature of the ARW model is slightly lower than that of the NMM model on the basis of WP-3 measurements. This may be one of the reasons which cause different model performances of ARW-CMAQ and NMM-CMAQ for $PM_{2.5}$ and its related chemical composition.

A comparison with the aircraft WP-3 observations reveals that both models generally estimated SO_4^{2-} well on most days except on 9/16 and 9/21 but consistently overestimated NH_4^+ vertically except at layer 1, whereas both models systematically underestimated the NH_3 vertically for all observations. Both models performed well for observed SO_4^{2-} and NH_4^+ made on 9/13 and 9/25 over the DFW. Both models generally estimated HNO_3 well on most days except on 9/15, 9/29 and 10/6 in which both models had consistently high HNO_3 and the means of observed and modeled SO_2 concentrations are close with general overestimations near ground and general underestimations at high altitudes. Both models have reasonable performance for isoprene at the low altitudes (<2000 m) but completely missed the observed isoprene at the high altitudes (>2000 m). There are consistent underestimations of terpenes by a factor of 2 to 4 by both models vertically from the low to high altitudes on most days especially at the high altitudes (> ~1500 m). Both models captured the observed toluene well although both models had slight overestimation near the ground and underestimation at the high altitudes (>~2000m). The systematical underestimation of terpene (by a factor of 2 to 4) suggests that the emission inventory may have been systematically low for terpene emissions. The time-series comparisons of the observations and models along the coast of southeastern Texas over the Gulf of Mexico show that both models captured the temporal variations and broad synoptic change seen in the observed HCHO and acetaldehyde with the means NMB <30% along the ship track most of the time but underestimated terpenes, isoprene, toluene and SO_2 consistently.

Given the fact that WRF-ARW and WRF-NMM use different dynamic cores which correspond to different sets of dynamic solvers that operates on a particular grid projection, grid staggering and vertical coordinate, it is not surprising that ARW-CMAQ and NMM-CMAQ showed some different as well as some similar model performances for $PM_{2.5}$, its chemical components and its related precursors, depending on the species and networks, as shown in this study. Since the significant differences between these two dynamic core meteorological forecasts are more the result of different physics but not dynamical core designs as summarized by Skamarock (2005), differences in the physics packages for WRF-ARW and WRF-NMM mainly cause the differences in ARW-CMAQ and NMM-CMAQ model performance as expected.

Acknowledgements

References

Bhave, P. V., S. J. Roselle, F. S. Binkowski, C. G. Nolte, S. C. Yu, G. L. Gipson, and K. L. Schere (2004), CMAQ aerosol module development: Recent enhancements and future plans, paper presented at 3rd Annual CMAS Models-3 Users' Conference, Commun. Model. and Anal. Syst. Cent., Chapel Hill, N. C., 18– 20 Oct.

Binkowski, F. S., and S. J. Roselle (2003), Models-3 Community Multiscale Air Quality (CMAQ) model aerosol component: 1. Model description, J. Geophys. Res., 108(D6), 4183, doi:10.1029/2001JD001409.

Carlton, A.G., B.J. Turpin, H.-J. Lim, and K.E. Altieri (2006), Link between isoprene and secondary organic aerosol (SOA): Pyruvic acid oxidation yields low volatility organic acids in clouds, *Geophys. Res. Lett*., 33, L06822, doi:10.1029/2005GL025374.

Cowling, E.B., Furiness, C., Dimitriades, B., and D. Parrish, D.: Final rapid science synthesis report: Findings from the second Texas air quality study (TexAQS II), TCEQ contract number 582-4-65614, 2007.

Dawson, J.P., Adams, P.J., and Pandis, S.N.: Sensitivity of $PM_{2.5}$ to climate in the Eastern US: a modeling case study. Atmos. Chem. Phys., 7, 4295-4309, 2007.

Department of Energy (DOE), Annual Energy Outlook 2006, DOE/EIA-0383, 2006

Edney, E.O., T.E. Kleindienst, M. Jaoui, M. Lewandowski, J.H. Offenberg, W. Wang, M. Claeys (2005), Formation of 2-methyl tetrols and 2-methylglyceric acid in secondary

organic aerosol from laboratory irradiated isoprene/NO_X/SO_2/air mixtures and their detection in ambient $PM_{2.5}$ samples collected in the eastern United States. *Atmos. Environ.,* 39, 5281-5289.

Federal Register (2006), National Ambient Air Quality Standards for Particulate Matter; Rule, RIN 2060-AI44, vol. 71, 61144, 17 Oct.

Grover, B. D., M. Kleinman, N. L. Eatough, D. J. Eatough, P. K. Hopke, R.W. Long,W. E.Wilson, M. B. Meyer, and J. L. Ambs (2005), Measurement of total PM2.5 mass (nonvolatile plus semivolatile) with the Filter Dynamic Measurement System tapered element oscillating microbalance monitor, J. Geophys. Res., 110, D07S03, doi:10.1029/2004JD004995.

Guenther, A., C. Geron, T. Pierce, B. Lamb, P. Harley, and R. Fall (2000), Natural emissions of non-methane volatile organic com-pounds; carbon monoxide, and oxides of nitrogen from North America, *Atmos. Environ.*, 34 (12–14), 2205–2230.

Janjic, Z. I.: A nonhydrostatic model based on a new approach. Meteorol. Atmos. Phys., 82, 271285, 2003..

McKeen, S.A., S.H. Chung, J. Wilczak, G. Grell, I. Djalalova, S. Peckham, W. Gong, V. Bouchet, R. Moffet, Y. Tang, G.R. Carmichael, R. Mathur, and S.C. Yu (2007), Evaluation of several PM2.5 forecast models using data collected during the ICARTT/NEAQS2004 field study. *J. Geophys. Res.*, 112 , D10S20, doi:10.1029/2006JD007608.

McKeen, S., Grell, G., Peckham, S., Wilczak, J., Djalalova, I., Hsie,, E. Y., Frost, G., Peischi, J., Schwarz, J., Spackman, R., Holloway, J., de Gouw, J., Warneke, C., Gong, W., Bouchet, V., Gaudreault, S., Racine, J., McHenry, J., McQueen, J., Lee, P., Tang, Y., Carmichael, G. R., and Mathur, R.: An evaluation of real-time air quality forecasts and their urban emissions over eastern Texas during the summer of 2006 Second Texas Air Quality field study. *J. Geophys. Res*., 114, D00F11, doi:10.1029/2008JD011697, 2009.

Morris, R.E., B. Koo, A. Guenther, G. Yarwood, D. McNally, T.W. Tesche, G. Tonneseon, J. Boylan, and P. Brewer (2006), Model sensitivity evaluation for organic

carbon using two multi-pollutant air quality models that simulate regional haze in the southeastern United States. *Atmos. Environ*., 40, 4960-4972.

Parrish, D. D., D. T. Allen, T. S. Bates, M. Estes, F. C. Fehsenfeld, G. Feingold, R. Ferrare, R. M. Hardesty, J. F. Meagher, J. W. Nielsen-Gammon, R. B. Pierce, T. B. Ryerson, J. H. Seinfeld, and E. J. Williams: Overview of the Second Texas Air Quality Study (TexAQS II) and the Gulf of Mexico Atmospheric Composition and Climate Study (GoMACCS). *J. Geophys. Res*., 114, D00F13, doi:10.1029/2009JD011842,2009

Skamarock,W. C., J. B. Klemp, J. Dudhia, D. O. Gill, D. M.Barker,W.Wang, and Powers, J.G.: A Description of the Advanced Research WRF Version 2. NCAR Technical Note NCAR/TND468+STR, Available at http://www.mmm.ucar.edu/wrf/users/docs/arw_v2.pdf, 2005

Skamarock,W. C.: Why is there more than one dynamical core in WRF? A technical perspective, Available at http://www.mmm.ucar.edu/people/skamarock/one_core_2005.pdf, 2005

Sisler, J. F., and W. C. Malm (2000), Interpretation of trends of PM2.5 and reconstructed visibility from the IMPROVE network, J. Air Waste Manage. Assoc., 50, 775– 789.

Turpin, B. J., and H.-J. Lim (2001), Species contributions to PM2.5 mass concentrations: Revisiting common assumptions for estimating organic mass, Aerosol Sci. Technol., 35, 602–610.

Wehner, B., and Wiedensohler, A.: Long term measurements of submicrometer urban aerosols: statistical analysis for correlations with meteorological conditions and trace gases. *Atmospheric Chemistry and Physics* **3**, 867-879, 2003

Whiteaker, J.R., Suess, D.T., and Prather K.A.: Effects of Meteorological Conditions on Aerosol Composition and Mixing State in Bakersfield, CA. *Environ. Sci. Technol.*, 36 (11), 345–2353, 2002.

Wise, E.K., and Comrie, A.C., : Meteorologically adjusted urban air quality trends in the Southwestern United States. Atmos. Environ., 39, 2969-2980, 2005.

Ying, Q., and Krishnan, A.: Source contributions of volatile organic compounds to ozone formation in southeast Texas. J. Geophys. Res., 115, D17306, doi:10.1029/2010JD013931, 2010.

Yu, S. C., P. S. Kasibhatla, D. L. Wright, S. E. Schwartz, R. McGraw, and A. Deng (2003), Moment-based simulation of microphysical properties of sulfate aerosols in the eastern United States: Model description, evaluation and regional analysis, J. Geophys. Res., 108(D12), 4353, doi:10.1029/2002JD002890.

Yu, S. C., R. Dennis, P. Bhave, and B. Eder (2004), Primary and secondary organic aerosols over the United States: Estimates on the basis of observed organic carbon (OC) and elemental carbon (EC), and air quality modeled primary OC/EC ratios, Atmos. Environ., 38, 5257– 5268.

Yu, S. C., R. Dennis, S. Roselle, A. Nenes, J. Walker, B. Eder, K. Schere, J. Swall, and W. Robarge (2005), An assessment of the ability of 3-D air quality models with current thermodynamic equilibrium models to predict aerosol NO3 _ , J. Geophys. Res., 110, D07S13, doi:10.1029/2004JD004718.

Yu, S.C., Eder, B., Dennis, R., Chu, S-H., and Schwartz, S.: New unbiased symmetric metrics for evaluation of air quality models. Atmospheric Science Letter, 7, 26-34, 2006.

Yu, S. C., P. V. Bhave, R. L. Dennis, and R. Mathur (2007), Seasonal and regional variations of primary and secondary organic aerosols over the continental United States: Semi-empirical estimates and model evaluation, Environ. Sci. Technol., 41, 4690– 4697.

Yu, S.C.,, Mathur, R., Schere, K., Kang, D., Pleim, J., Young, J., Tong, D., McKeen, S., and Rao, S.T.: Evaluation of real-time $PM_{2.5}$ forecasts and process analysis for $PM_{2.5}$ formation over the eastern U.S. using the Eta-CMAQ forecast model during the 2004 ICARTT Study. J. Geophys. Res., 113, D06204, doi:10.1029/2007JD009226, 2008.

Yu, S. C., Mathur, R., Pleim, J., Pouliot, G., Wong, D., Eder, B., Schere, K., Gilliam, R., and Rao, S. T.: Comparative evaluation of the impact of WRF-NMM and WRF-ARW meteorology on CMAQ simulations for O3 and related species during the 2006

TexAQS/GoMACCS campaign, Atmos. Poll. Res., doi:10.5094/APR.2012.015, 2011.

Zhang, Y., Pun, B., Vijayaraghavan, K., Wu, S.Y., Seigneur, C., Pandis, S.N., Jacobson, M.Z., Nenes, A., and Seinfeld, J.H.: Development and application of the model of aerosol dynamics, reaction, ionization, and dissolution (MADRID), J. Geophys. Res., 109, D01202, doi:10.1029/2003JD003501, 2004.

Table 1. Comparison of ARW-CMAQ and NMM-CMAQ models for operational evaluation of daily PM2.5 concentrations on the basis of the AQS data over the eastern United States

| | Number | Domain Mean, $\mu g\ m^{-3}$ | | | RMSE, $\mu g\ m^{-3}$ | | MB, $\mu g\ m^{-3}$ | | NMB (%) | | NME (%) | | R | |
		Obs	ARW	NMM	ARW	NMM	ARW	NMM	ARW	NMM	ARW	NMM	ARW	NMM
Rural	4103	12.8	10.0	8.1	6.9	7.9	-2.8	-4.7	-21.9	-36.9	38.8	45.5	0.63	0.60
Suburban	6554	13.6	13.6	11.2	7.7	7.7	0.0	-2.3	0.2	-17.2	39.4	40.9	0.56	0.52
Urban	5299	13.2	13.5	11.2	8.1	7.8	0.4	-2.0	2.8	-15.4	41.7	42.2	0.53	0.50
All data	19168	12.3	12.2	10.0	7.9	7.6	-0.1	-2.3	-0.4	-18.4	43.7	44.3	0.53	0.51

Table 2. Comparison of ARW-CMAQ and NMM-CMAQ models for PM2.5 and its components for each network over the eastern United States during the 2006 TexAQS/GoMACCS period.

	CASTNet					IMPROVE						STN				
	SO_4^{2-}	NH_4^+	NO_3^-	SO_2	TotS	$PM_{2.5}$	SO_4^{2-}	NO_3^-	OC	EC	TC	$PM_{2.5}$	SO_4^{2-}	NH_4^+	NO_3^-	TC
									ARW-CMAQ							
Mean (Obs)	4.16	1.26	0.32	0.72	2.42	7.19	2.48	0.22	1.24	0.31	1.55	13.49	3.86	1.32	0.56	4.32
Mean (Model)	3.74	1.23	0.47	1.45	3.31	7.14	2.88	0.38	1.11	0.28	1.38	15.53	4.90	1.91	1.12	3.23
Number	500	500	500	500	500	1648	1169	1169	1628	1628	1628	1816	1945	1945	1854	1971
correlation	0.88	0.82	0.30	0.73	0.81	0.52	0.64	0.35	0.30	0.48	0.37	0.30	0.57	0.45	0.36	0.29
MB	-0.41	-0.03	0.15	0.72	0.89	-0.05	0.40	0.16	-0.13	-0.04	-0.17	2.04	1.04	0.59	0.56	-1.09
RMSE	1.46	0.52	0.60	1.09	1.58	6.25	2.62	0.92	1.27	0.58	1.71	11.10	3.38	1.49	1.54	2.74
NMB (%)	-9.9	-2.5	46.7	99.4	36.8	-0.7	16.3	71.4	-10.7	-11.8	-10.9	15.1	27.0	100.6	44.8	-25.1
NME (%)	24.5	29.9	115.7	105.6	45.3	56.1	64.2	165.0	65.5	67.4	63.1	57.2	62.2	159.4	80.0	47.8
									NMM-CMAQ							
Mean (Obs)	4.16	1.26	0.32	0.72	2.42	7.19	2.48	0.22	1.24	0.31	1.55	13.49	3.86	1.32	0.56	4.32
Mean (Model)	2.94	0.99	0.43	1.36	2.93	5.85	2.04	0.37	1.00	0.22	1.22	11.32	3.33	1.33	0.74	2.52
Number	500	500	500	500	500	1648	1169	1169	1628	1628	1628	1816	1945	1945	1854	1971
correlation	0.89	0.83	0.23	0.77	0.83	0.61	0.77	0.39	0.42	0.53	0.46	0.35	0.66	0.54	0.36	0.37
MB	-1.22	-0.27	0.10	0.64	0.50	-1.34	-0.44	0.15	-0.24	-0.09	-0.33	-2.17	-0.53	0.01	0.19	-1.80
RMSE	1.98	0.60	0.52	0.93	1.20	5.02	1.93	0.77	1.06	0.44	1.38	9.53	2.50	1.03	1.00	2.75
NMB (%)	-29.3	-21.6	32.2	87.9	20.8	-18.6	-17.7	69.5	-19.7	-28.4	-21.5	-16.1	-13.7	0.4	33.3	-41.8
NME (%)	33.0	32.9	103.3	94.5	34.1	45.7	43.9	157.9	56.5	60.2	54.5	46.4	43.6	53.0	106.5	52.9

* The unit of Mean, MB, RMSE is $\mu g\ m^{-3}$, and TotS is total sulfur ($SO_4^{2-} + SO_2$) concentrations ($\mu g\ S\ m^{-3}$).

Table 3. Flight Observation Summary for WP-3 aircraft for PM during the 2006
TexAQS/GoMACCS study

Date	Observation summary for WP-3[*]
9/13	Dallas emission characterization and chemical processing, mean flow wind speed is 5 m/s with northerly wind, takeoff at 10:45 and landing at 16:45 (LST)
9/15	Houston Urban, Parish power plant, Isolated refineries, light winds, Emission characterization, chemical processing, mean flow wind speed is 4.5 m/s with southeasterly wind, takeoff at 9:50: and landing at 16:20 (LST)
9/16	Houston emission characterization and chemical processing, NE Texa power plants and aged Houston plume, takeoff at 9:55 and landing at 16:30 (LST)
9/19	Houston Urban, Parish power plant, Isolated refineries, flow from the NE, Emission characterization, chemical processing, mean flow wind speed is 7.5 m/s with northeasterly wind, takeoff at 9:50 and landing at 16:20 (LST)
9/20	Beaumont Port Arthur, Houston Urban, Parish power plant, Isolated refineries, emission characterization, chemical processing, mean flow wind speed is 5.0 m/s with easterly wind, takeoff at 9:55 and landing at 16:15 (LST)
9/21	Houston Urban and Industrial, Parish power plant, emission characterization, chemical processing, mean flow wind speed is 9.5 m/s with southerly wind, takeoff at 9:50 and landing at 16:25 (LST)
9/25	Dallas, Parish power plant, Big Brown and Limestone power plants, GMD tower, emission characterization, chemical processing, mean flow wind speed is 3.5 m/s with northerly wind, takeoff at 9:45 and landing at 16:25 (LST)
9/27	Houston Urban & Industrial, Parish power plant, Beaumont-Port Arthur, emission characterization, chemical processing, mean flow wind speed is 3.5 m/s with southerly wind, takeoff at 12:45 and landing at 17:55 (LST)
9/29	Houston Urban & Industrial, Parish power plant, Emission characterization, chemical processing into the night, mean flow wind speed is 7.0 m/s with southeasterly wind, takeoff at 13:45 and landing at 20:10 (LST)
10/5	Houston Urban & Industrial, Parish power plant, Chemical processing and transport, light winds from the northeasterly, takeoff at 9:50 and landing at 16:20 (LST)
10/6	Houston Urban & Industrial, Parish power plant, Victoria and Seadrift, chemical processing and transport, winds from the northeasterly, takeoff at 9:50 and landing at 16:00 (LST)

* based on flight information presented at http://esrl.noaa.gov/csd/tropchem/2006TexAQS/P3/index.html and
    McKeen et al (2009).

Table 4. Comparison of layer means of $PM_{2.5}$ (SO_4^{2-} and NH_4^+) and its related precursors from observations and model (ARW-CMAQ, NMM-CMAQ) on the basis of all P3 aircraft measurements during the 2006 TexAQS/GoMACCS.

		SO_4^{2-}		NH_4^+		HNO_3		NH_3		SO_2		isoprene		toluene		terpenes	
Layer	Height	obs	Mod	obs	Mod	obs	Mod	obs	Mod	obs	Mod	obs	Mod	obs	Mod	obs	Mod
								ARW-CMAQ									
1	38	2.80	1.69	0.82	0.72	1.75	2.20	2.37	1.12	2.74	3.63	475.0	304.4	355.5	518.8	87.3	41.2
2	79	0.95	0.65	1.40	1.68	1.74	2.30	2.04	0.97	2.62	3.84	315.4	272.1	260.1	462.7	48.0	40.5
3	118	1.03	2.13			1.92	2.31	2.07	0.76	2.52	3.40	185.3	161.2	358.8	251.9	49.4	18.5
4	158					2.02	2.33	2.39	0.71	2.68	2.84	270.3	173.6	408.9	322.2	36.4	16.8
5	239	2.93	3.25	1.15	1.42	1.84	2.22	2.06	0.55	2.15	2.12	237.2	163.9	247.5	174.9	33.0	12.9
6	319	3.22	3.07	1.22	1.57	1.79	2.60	1.91	0.42	2.05	1.46	209.5	149.4	143.5	129.1	33.3	9.5
7	401	3.31	3.33	0.85	1.10	2.12	2.49	1.43	0.71	1.68	1.36	298.7	300.4	173.6	137.3	41.6	26.4
8	482	2.91	2.81	0.76	0.97	2.02	2.49	1.48	0.58	1.97	1.65	188.8	154.2	169.5	140.9	35.2	11.8
9	565	3.19	2.85	0.80	1.02	1.80	2.44	1.25	0.41	1.73	1.36	157.5	142.3	126.5	100.2	31.1	9.0
10	648	2.83	2.89	0.54	0.89	1.69	2.33	1.15	0.48	1.52	1.02	172.3	139.9	127.4	95.3	32.4	10.0
11	731	2.63	3.03	0.62	0.86	1.61	1.99	1.13	0.54	1.48	0.96	158.9	156.8	120.5	84.5	34.3	11.5
12	815	2.68	2.76	0.60	0.93	1.64	2.04	1.09	0.49	1.45	1.01	127.7	128.1	121.9	76.5	31.0	9.6
13	985	2.45	3.20	0.47	0.80	1.56	1.99	1.00	0.50	1.34	1.11	126.7	109.2	95.5	89.5	33.4	7.7
14	1158	2.99	2.90	0.54	0.96	1.59	2.48	0.80	0.49	1.54	1.19	138.9	165.7	92.7	103.1	27.7	11.5
15	1333	2.84	2.49	0.57	0.96	1.25	2.08	0.64	0.42	0.81	0.90	104.2	133.8	77.2	87.8	26.1	9.6
16	1511	2.13	2.18	0.71	0.92	1.01	1.65	0.53	0.32	0.71	0.67	62.5	58.5	46.4	54.5	24.8	3.8
17	1692	1.51	1.78	0.39	1.13	0.83	1.51	0.46	0.21	0.48	0.55	48.7	33.3	45.8	41.3	27.5	3.3
18	1968	1.85	2.52	0.50	0.68	0.70	1.32	0.39	0.20	0.41	0.51	35.9	25.6	39.7	32.4	19.5	1.7
19	2252	1.51	1.73	0.40	0.65	0.52	0.96	0.30	0.12	0.28	0.35	35.1	3.6	31.2	13.5	21.5	0.2
20	2643	2.31	2.53	0.39	0.47	0.39	0.77	0.24	0.05	0.25	0.23	29.8	0.6	22.4	10.4	17.4	0.0
21	3155	0.58	0.77	0.28	0.39	0.35	0.65	0.21	0.08	0.24	0.15	30.7	0.9	23.8	7.4	20.6	0.0
22	3695	1.57	0.81	0.41	0.47	0.26	0.46	0.18	0.01	0.25	0.07	35.2	0.1	25.0	5.5	21.8	0.0
23	4265			0.10	0.10	0.17	0.34	0.16	0.00	0.24	0.02	43.6	0.5	23.9	4.9	25.2	0.0
24	4872			1.00	0.16	0.13	0.28	0.06	0.00	0.27	0.02	42.6	1.4	22.2	2.4	21.9	0.1
25	5523					0.08	0.22	0.15	0.00	0.30	0.01	45.4	1.4	21.5	2.1	23.3	0.2
mean		2.30	2.35	0.66	0.86	1.23	1.70	1.02	0.41	1.27	1.22	143.0	111.2	127.2	118.0	32.1	10.2
								NMM-CMAQ									
1	38	2.61	1.10	0.82	0.63	1.74	2.22	2.37	1.06	2.72	4.11	471.0	302.0	354.0	547.0	83.7	45.9
2	116	1.10	1.56	1.40	1.64	1.88	2.36	2.04	0.76	2.54	3.69	225.0	161.0	386.0	308.0	48.3	18.4
3	197	2.58	2.13			1.88	2.46	2.29	0.63	2.27	2.73	259.0	139.0	266.0	203.0	34.5	12.5
4	282	3.07	3.09	0.94	1.25	1.88	2.48	1.93	0.46	1.91	1.63	204.0	118.0	146.0	112.0	32.7	7.5
5	372	2.31	2.50	0.73	1.12	2.01	2.72	1.46	0.49	1.73	1.22	276.0	221.0	176.0	118.0	38.5	21.7
6	470	2.68	2.67	0.79	1.00	2.05	2.59	1.46	0.51	1.97	1.36	189.0	132.0	165.0	122.0	34.8	11.1
7	578	2.78	2.69	0.80	1.10	1.64	2.55	1.19	0.43	1.65	1.19	188.0	152.0	129.0	96.7	32.5	11.9
8	699	2.03	2.79	0.54	0.91	1.74	2.44	1.16	0.44	1.60	1.11	149.0	113.0	138.0	102.0	31.7	9.2
9	847	2.55	2.56	0.59	0.97	1.57	2.02	1.06	0.40	1.33	0.91	128.0	104.0	108.0	80.6	39.0	8.5
10	1049	2.49	2.65	0.45	0.85	1.65	2.73	0.91	0.41	1.48	1.15	138.0	106.0	103.0	116.0	26.7	8.1
11	1301	3.55	2.79	0.60	1.09	1.22	2.26	0.64	0.32	0.92	0.78	104.0	85.7	71.9	71.6	28.0	6.4
12	1753	1.32	2.00	0.46	0.99	0.84	1.42	0.46	0.21	0.52	0.43	47.7	37.5	44.8	34.2	25.3	3.3
13	2283	1.70	1.77	0.42	0.69	0.53	0.89	0.29	0.09	0.31	0.22	32.8	9.3	31.7	14.3	19.1	0.8
14	2898	1.72	1.04	0.39	0.57	0.36	0.61	0.22	0.06	0.25	0.16	31.0	2.0	24.0	6.8	19.7	0.1
15	3619			0.37	0.46	0.25	0.35	0.16	0.01	0.26	0.10	34.9	0.1	25.3	2.1	21.9	0.0
16	4460			0.55	0.11	0.16	0.23	0.06	0.00	0.25	0.03	46.6	0.0	23.0	1.3	24.1	0.0
17	5413					0.11	0.15	0.12	0.00	0.29	0.01	39.6	0.0	23.4	0.6	22.9	0.0
mean		2.32	2.24	0.66	0.89	1.26	1.79	1.05	0.37	1.29	1.22	150.8	99.0	130.3	113.9	33.1	9.73

* $\mu g\ m^{-3}$: SO_4^{2-} and NH_4^+; ppbv: HNO_3, NH_3, SO_2; pptv: isoprene, toluene, terpenes; m: height.

Table 5. Comparison of observations and models (NMM-CMAQ and ARW-CMAQ) for different gaseous species (SO_2, NH_3, acetaldehyde, formaldehyde, isoprene, toluene and terpenes) on the basis of all ship measurements over the Gulf of Mexico during the 2006 TexAQS (all units are ppbv).

| | Mean ± standard deviation | | | NMB (%) | |
	Obs	NMM-CMAQ	ARW-CMAQ	NMM-CMAQ	ARW-CMAQ
SO2	3.77±9.83	2.66±3.94	2.12±3.37	-29.5	-43.7
NH3	0.41±1.73	0.53±1.08	0.50±1.14	29.0	22.2
Acetaldehyde	1.00±1.06	1.35±1.37	1.29±1.31	34.6	29.0
Formaldehyde	2.01±2.03	2.45±1.88	2.28±1.69	21.6	13.0
Isoprene	0.35±0.57	0.19±0.34	0.23±0.50	-45.6	-34.0
Toluene	0.61±1.40	0.41±0.53	0.37±0.60	-32.8	-38.8
Terpenes	0.25±0.23	0.06±0.11	0.05±0.10	-74.2	-80.9
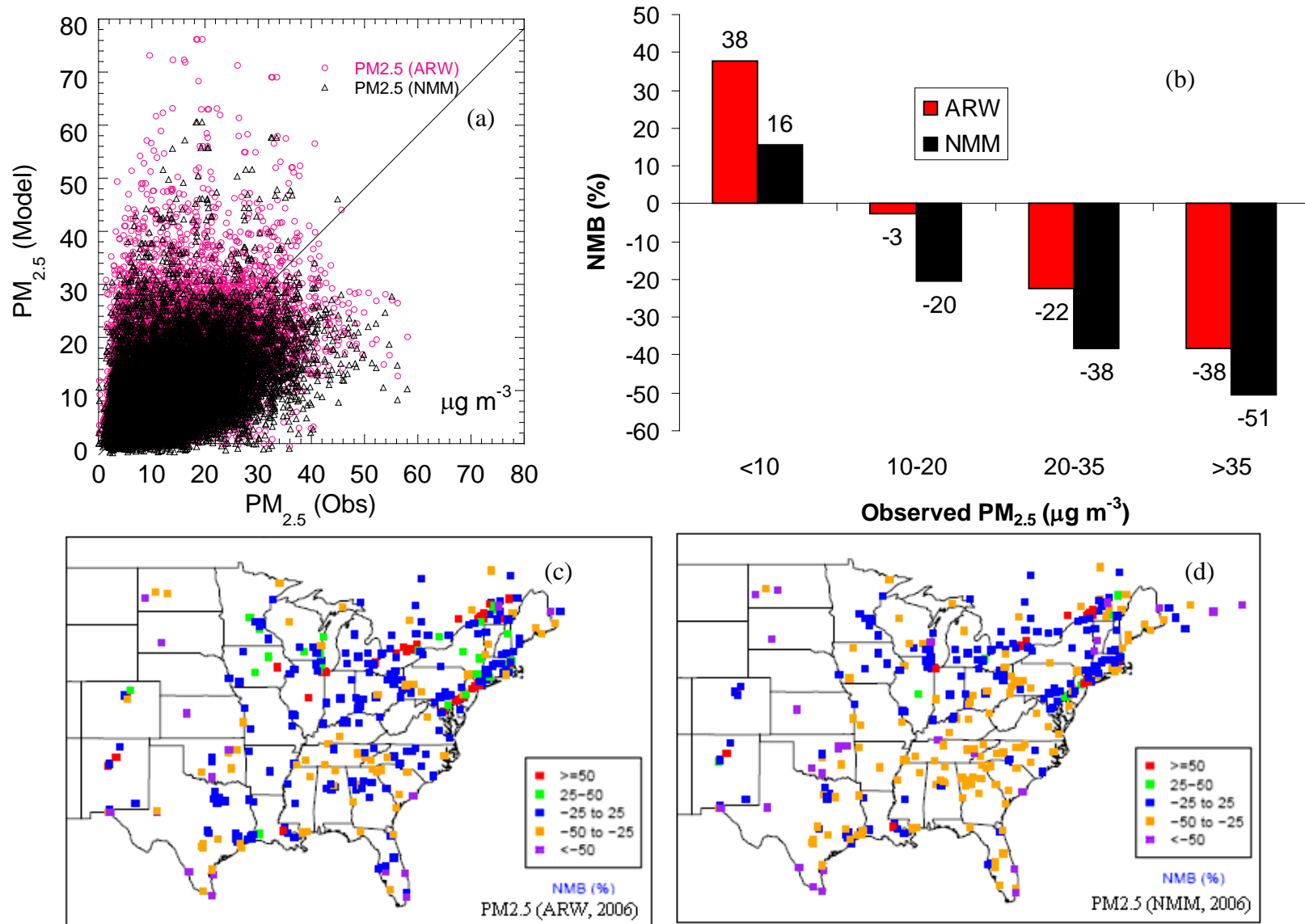
Figure 1. Comparison of the modeled (ARW-CMAQ, NMM-CMAQ) and observed daily PM$_{2.5}$ concentrations at the AIRNow monitoring sites (a)scatterplot (ppbv); (d) The NMB values of each model as a function of the observed daily PM$_{2.5}$ concentration ranges; spatial distributions of NMB for (c) ARW-CMAQ and (d) NMM-CMAQ during the period 5 August and 7 October, 2006.
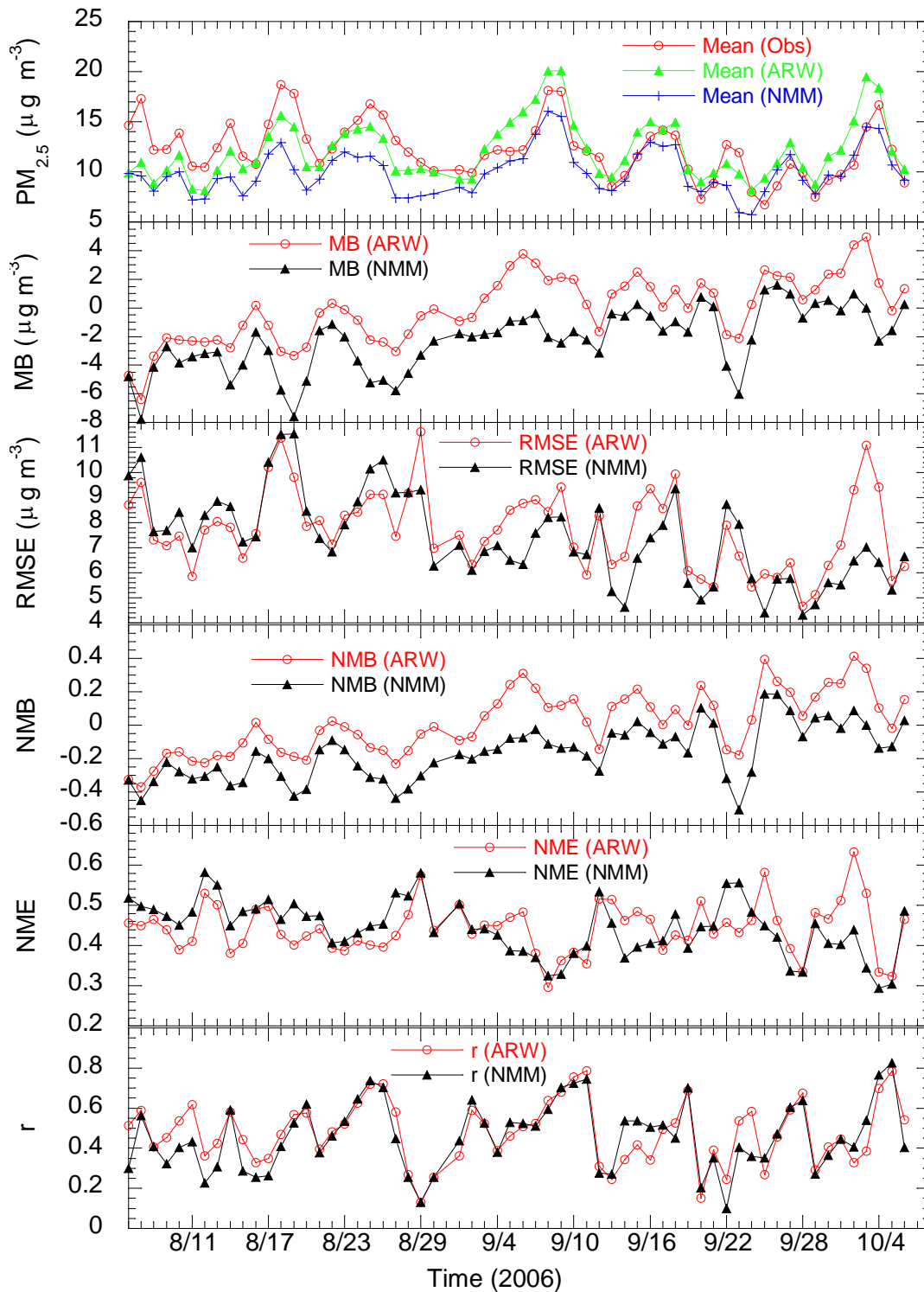
Figure 2. Comparison of daily variations of the values of domain-wide mean, MB, RMSE, NMB, NME and correlation coefficient (r) for the daily $PM_{2.5}$ mass concentrations at the AIRNow monitoring sites for ARW-CMAQ and NMM-CMAQ simulations.
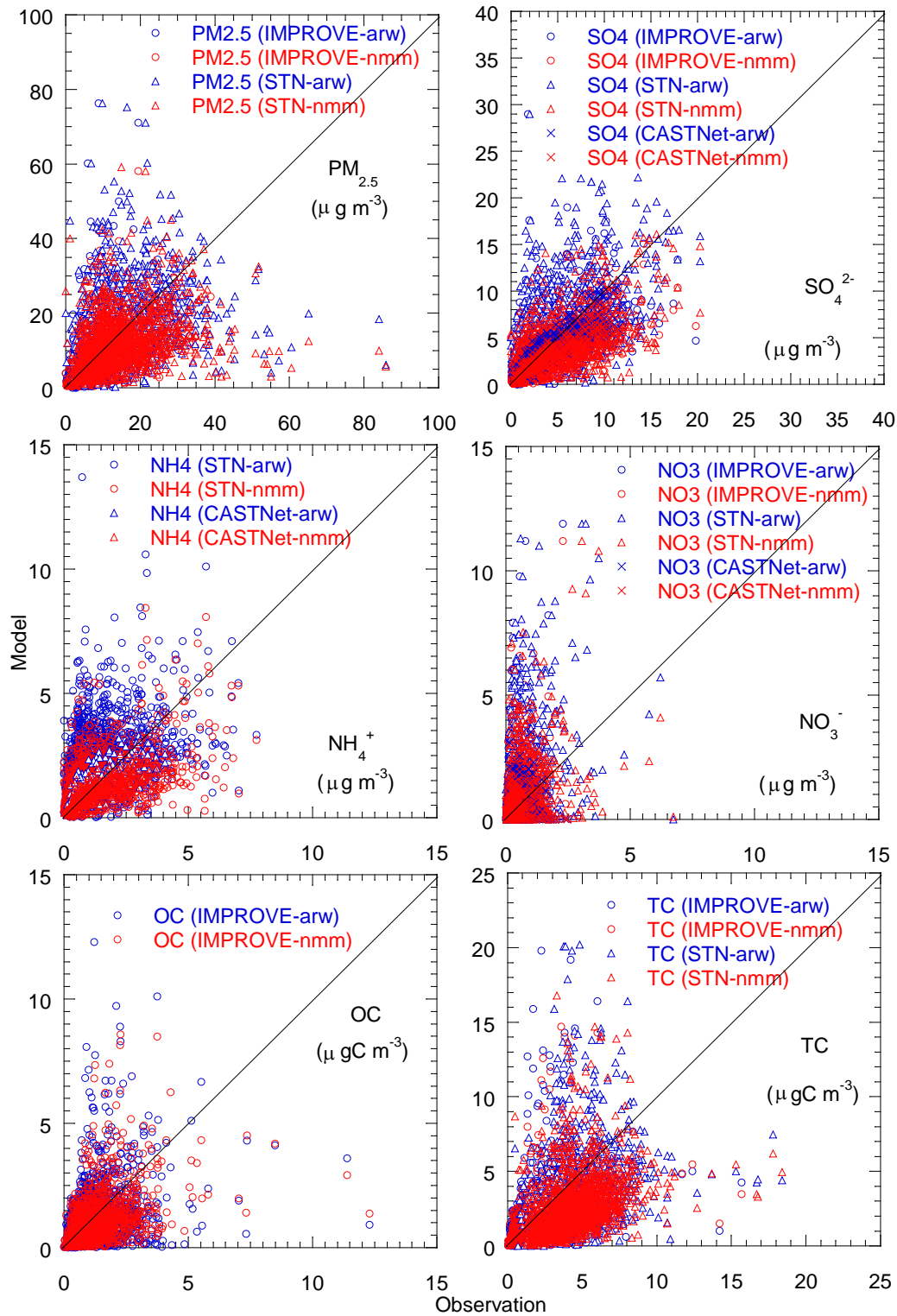
Figure 3a. Comparison of observed and modeled (ARW-CMAQ and NMM-CMAQ) PM$_{2.5}$ and its chemical composition at the IMPROVE, STN and CASTNet sites during the 2006 TexAQS/GoMACCS period
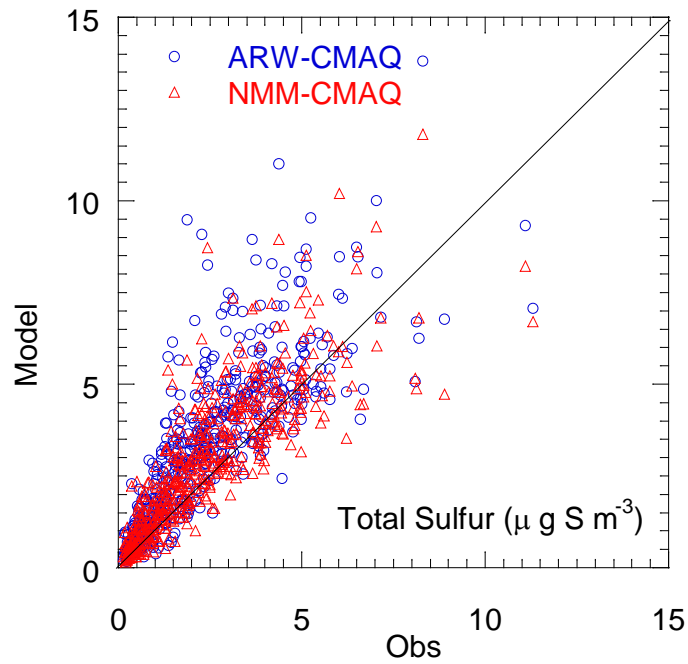
Figure 3b. Comparison of observed and modeled (ARW-CMAQ and NMM-CMAQ) total sulfur (SO_4^{2-} + SO_2) concentrations at the CASTNet sites during the 2006 TexAQS/GoMACCS period.
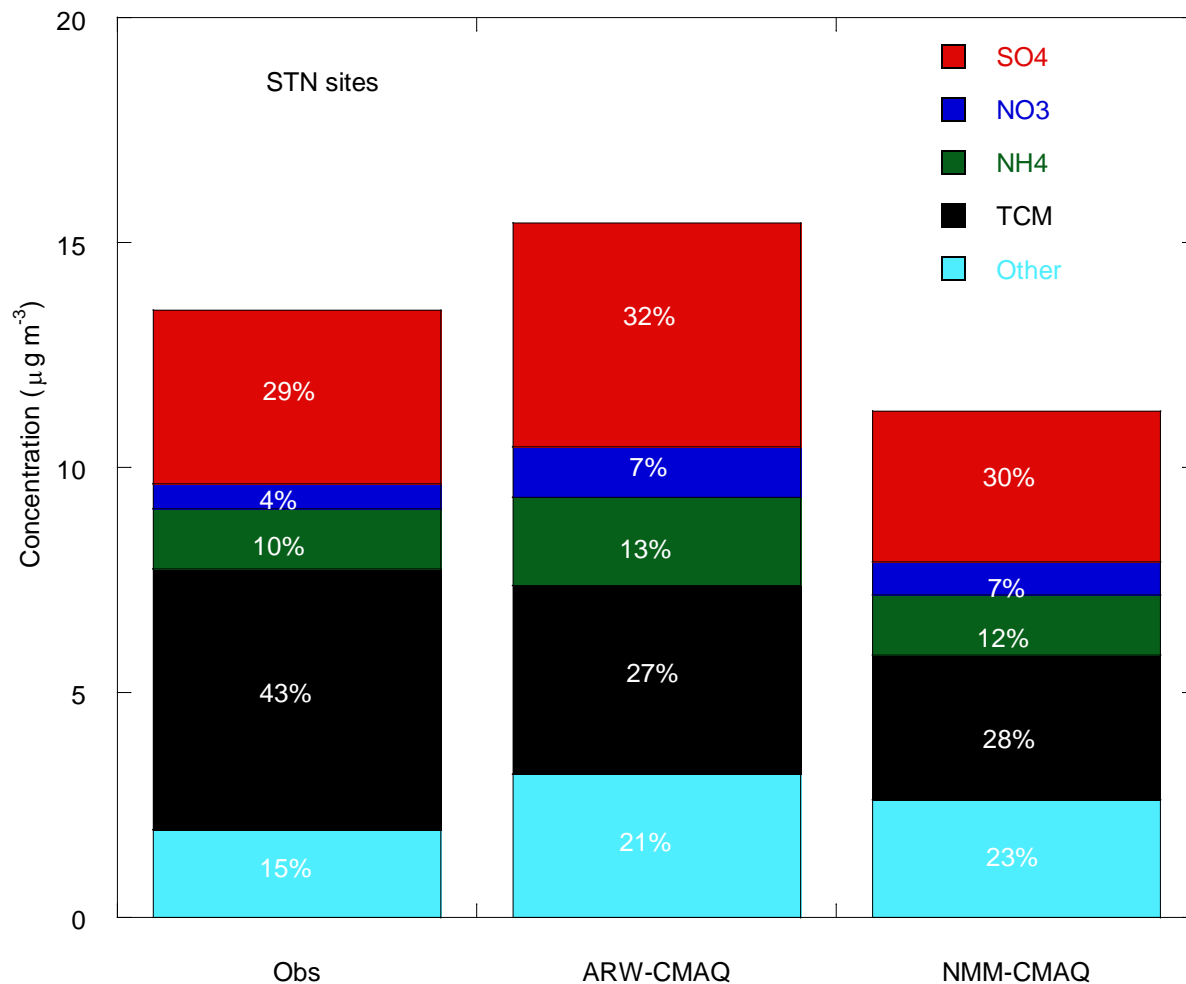
Figure 4. Comparison of stacked bar-plots for observed and modeled (ARW-CMAQ, NMM-CMAQ) $PM_{2.5}$ chemical composition at the STN sites during the 2006 TexAQS/GoMACCS period. The percentages represent the fractions of each composition for $PM_{2.5}$. "OTHER" species refers to unspecified anthropogenic mass which comes from the emission inventory of $PM_{2.5}$.
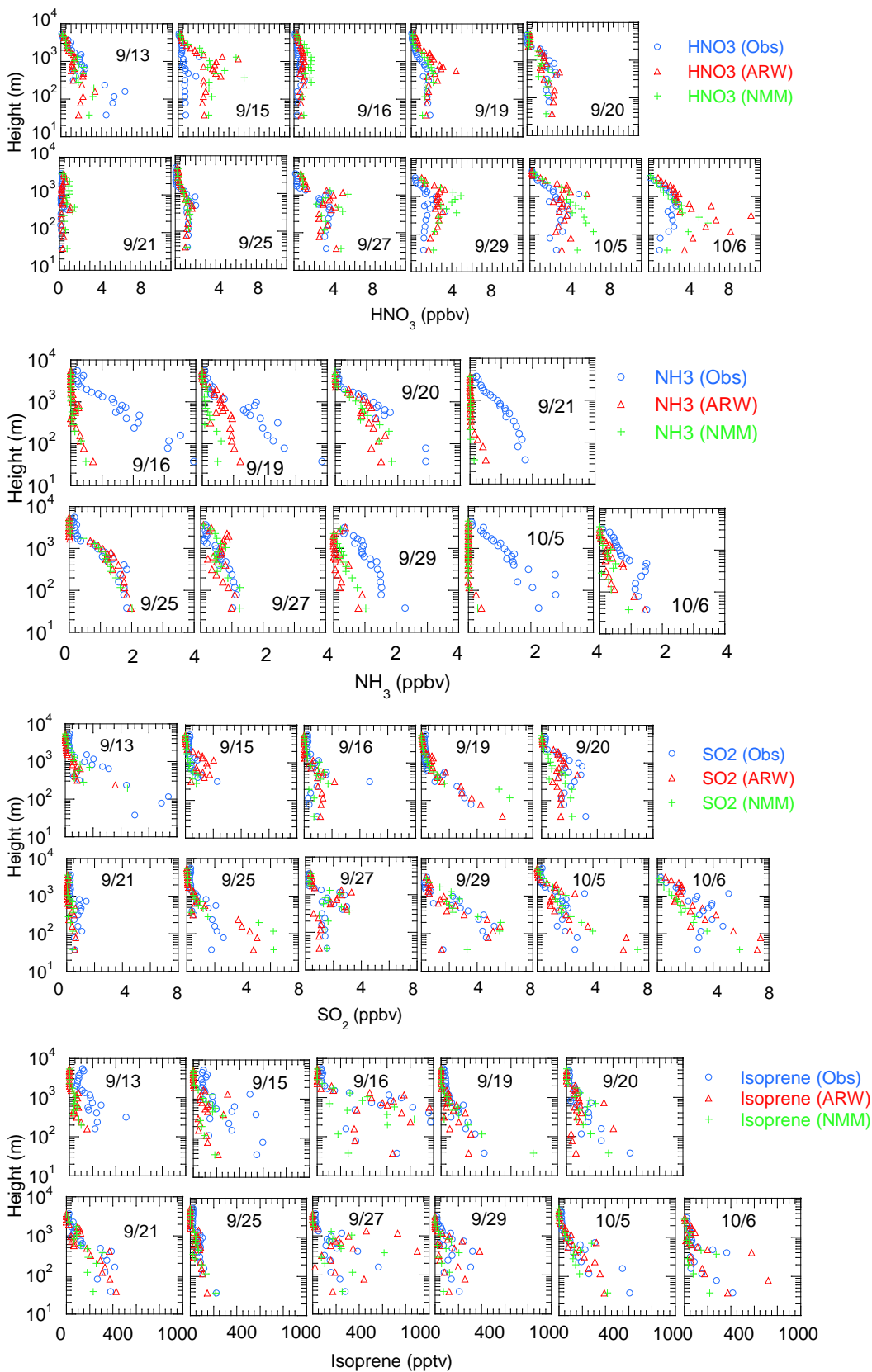
Figure 5. Comparison of composite vertical distributions of observed and modeled (ARW-CMAQ and NMM-CMAQ) HNO_3, NH_3, SO_2, Isoprene, toluene, terpenes, $PM_{2.5}$ SO_4^{2-} and NH_4^+ along the aircraft transects of WP-3 during the 2006 TexAQS/GoMACCS.
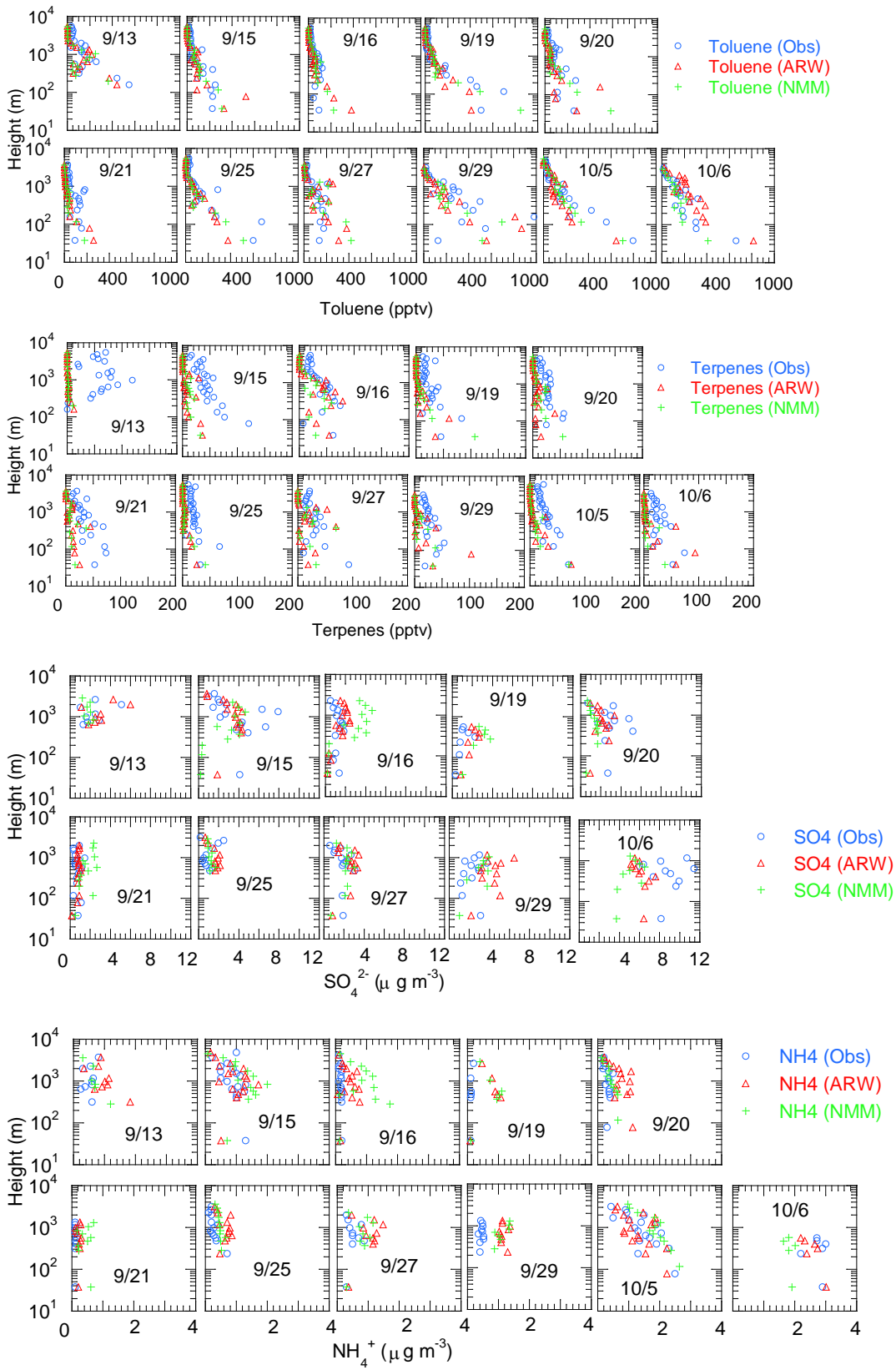
Figure 5. (Continued)
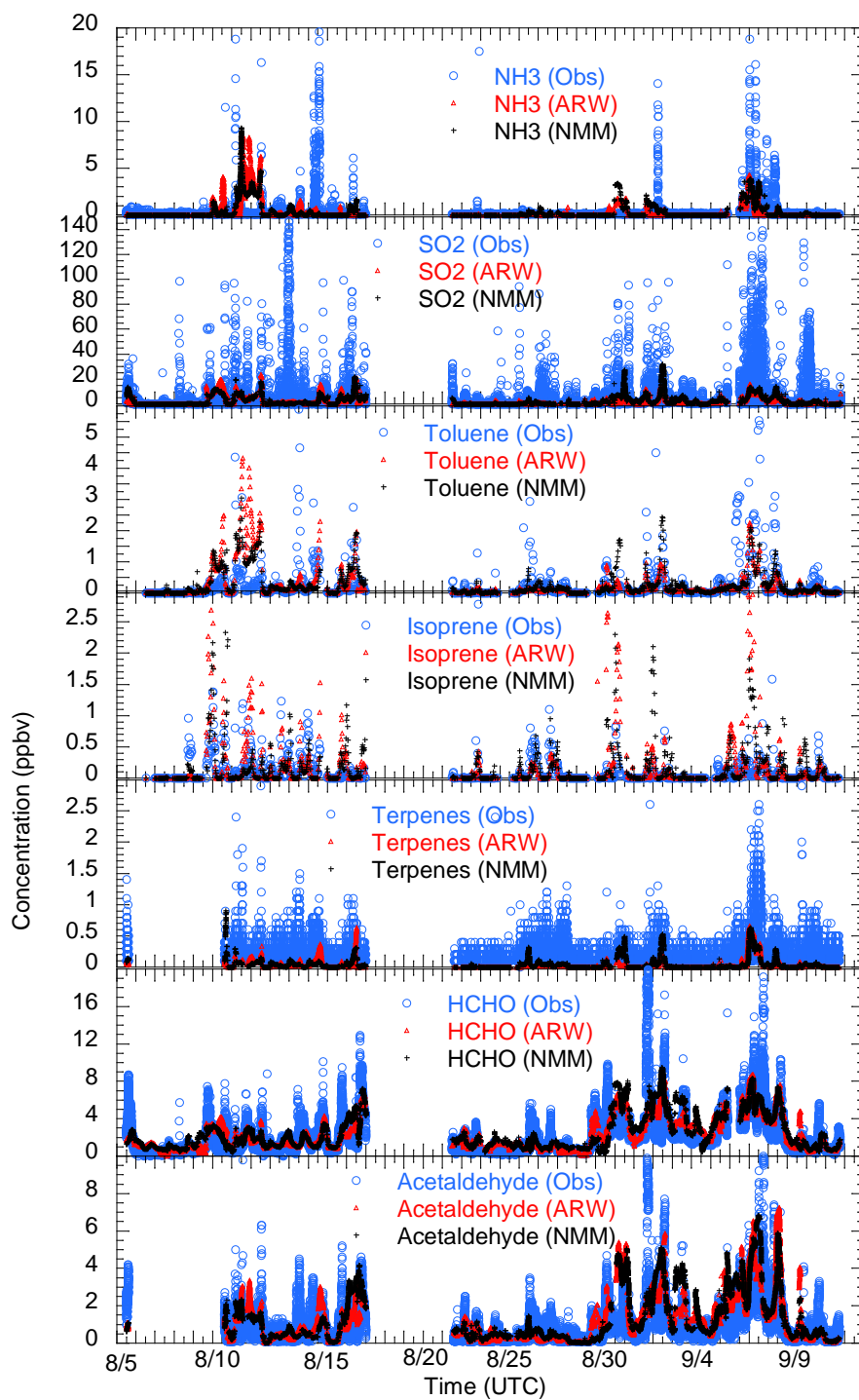
Figure 6. Time series of observations and model predictions (NMM-CMAQ and ARW-CMAQ) for difference species on the basis of ship measurements over the Gulf of Mexico during the 2006 TexAQS/GoMACCS period.